# *Magnetic Small-angle Neutron Scattering*

# 1. Introduction

## 1.1 Overview

Small Angle Neutron Scattering (SANS) is a technique that allows characterizing structures or objects on the nanometer scale, typically in the range between 1 nm and 150 nm. The information one can extract from SANS is primarily the average size, size distribution and spatial correlation of nanoscale structures, as well as shape and internal structure of particles (e.g. core-shell structure). Further, the scattering intensity on an absolute scale contains the product of scattering contrast of the investigated structures in the surrounding medium, and number or volume density. If one of both quantities is known, the other one can be derived in addition to the information mentioned before. All in all, SANS is a valuable technique, widely used in many fields, to characterize particles (in solution or in bulk), clusters, (macro-)molecules, voids and precipitates in the nanometer size range. Further, in-situ measurements allow following the temporal development and dynamics of such structures, on a time scale ranging from microseconds (stroboscopic) to hours.

Besides the nuclear interaction, due to their magnetic moment neutrons undergo a magnetic interaction with matter, approximately equally strong (in terms of order of magnitude) as the nuclear interaction. This property distinguishes neutrons markedly from x-rays where magnetic interaction is very weak and difficult to access experimentally. With this dual interaction of neutrons with matter they offer the opportunity to study both, compositional and magnetic structures and correlations. Thus, a strong area of application of neutrons traditionally was and still is the area of magnetism in solid state physics and condensed matter research. SANS in particular, probing structures on the nanometer scale, finds applications in micromagnetism, to magnetic clusters embedded in a solid nonmagnetic matrix, magnetic clusters suspended in fluids (e.g. ferrofluids), magnetism in nanostructured materials, vortex lattices in superconductors and many others. Further, by using a polarized neutron beam, very specific information on the magnetic structure or alignment of nanoparticles can be obtained, as well as on their response to an external magnetic field. In general, neutrons are the only probe which give direct access to magnetic moments and magnetic interactions and alignment down to the atomic scale, and the probing does not by itself impose a magnetic perturbance, as e.g. by an external magnetic field.

## 1.2 The classical SANS instrument

The classical concept of a SANS instrument at a continuous neutron source was first realised in the early 1970's at the Jülich Research Centre, Germany, the ILL Grenoble, France [4] and the HFIR reactor in Oak Ridge, USA [5]. Modern instruments of this type, like the D22 instrument at the ILL, the SANS at HMI, Berlin, Germany, or the SINQ-SANS at PSI, Switzerland [6], still follow the same principle concept, although using state-of-the-art components and advanced technical concepts. For measurements of magnetic structures polarisation and spin-flipping of the incident beam is a viable option at HZB [7], ML Munich (D) [x], NIST, Gaithersburg (USA) LLB, Saclay (F) [9] and PSI, Villigen (CH).

The basic layout of a classical SANS instrument is illustrated in Figure 1. The preferential position of the instrument is at the end of a neutron guide supplying a spectrum of cold neutrons. The neutron energy, or wavelength, respectively, is selected by a mechanical velocity selector with a resolution of typically 10% FWHM. Double pin-hole collimation tailors the beam for the necessary angular resolution, and a two-dimensional position sensitive detector registers the neutrons which are scattered to small angles around the incoming beam. The favored instrument is typically 40 m in length, 20 m for the collimation and 20 m for the secondary flight path with a flexible distance between sample position and detector. The detector sizes nowadays reach 96x96 $cm^2$ with about 16000 pixels of 7.5x7.5 $mm^2$ resolution. Electromagnets, cryomagnets, furnaces and cryostats, alone or in combination, belong generally to the standard equipment for sample environments.

At a pulsed source, like ISIS (UK) or IPNS (USA) [10], the concept of a SANS instrument is different, making use of a time-of-flight selection of the 'white' incoming beam. Besides that, the operational concept is very similar to instruments at continuous sources.

In the experiment the scattered intensity is registered as a function of the radial distance from the beam center, i.e. as a function of the scattering angle $2\theta$, or, more general, as function of the scattering vector **Q** or of its modulus $Q$. The latter is related to $2\theta$ via $Q = (4\pi/\lambda) \sin \theta$, with $\lambda$, the neutron wavelength. By appropriate calibration one obtains the intensity in absolute units of the differential scattering cross section $(d\sigma/d\Omega)$ $(Q)$. When the scattering is isotropic around the central beam, it may be averaged azimuthally for each value of $Q$ (so-called "radial average"). If the scattering is non-isotropic, as often observed in the case of magnetic scattering, one has to consider the scattering in different azimuthal directions by sectional averaging.

For characterizing magnetic structures it is mostly necessary, or at least helpful, to analyze the response of the scattering to an externally applied magnetic field. In the examples in this practical such an external field, when applied, is assumed to be homogeneous, directing horizontally and perpendicular to the incident neutron beam. Other configurations are possible and can be adapted if appropriate, for instance, a beam-parallel field for investigating vortex lattices in superconductors. Such examples are not considered here, although the same theoretical principles as outlined in section 2 apply.

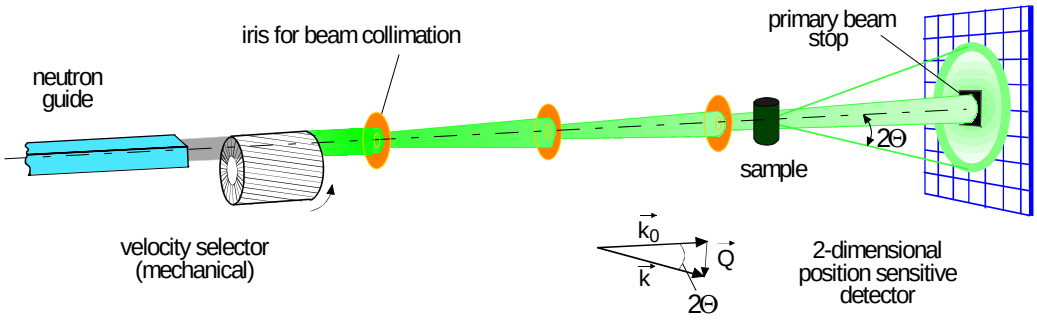


Figure 1: Schematic layout of a classical SANS facility at a continuous neutron source.

# 2. Neutron scattering

This section gives a general theoretical introduction to neutron scattering focusing to magnetic scattering and small angle scattering, with the objective to introduce the established notations and present and explain the most important basic formulae needed to evaluate a scattering experiment characterizing magnetic structures. For further reading and more details we refer to [11-20].

In a scattering experiment, the primary goal is a detailed analysis of the measured scattering pattern in relation to the properties of the incoming neutron beam. Monochromator and collimator define the energy (wavelength) and divergence of the incoming neutrons. Those interact with a sample and thereby undergo a momentum transfer $\hbar\mathbf{Q}$, with the scattering vector $\mathbf{Q}=\mathbf{k}_0-\mathbf{k}$, and $\mathbf{k}_0$, $\mathbf{k}$ being the wave vectors of the incoming and scattered neutrons, respectively. This process in principle can be elastic or inelastic. For small angle scattering inelastic scattering events are of minor importance and will be neglected in the present treatise.

## 2.1 Scattering potential

The scattering of a neutron, interacting through a scalar potential $V(\mathbf{r})$ with material, can be described by the asymptotic solution of the Schrödinger equation, see e.g. [11,12], which results in the wave function

$$\varphi_{\mathbf{k}_0}(\mathbf{r}) \xrightarrow[\mathbf{r}\to\infty]{} \frac{1}{(2\pi)^{3/2}}\left[e^{i\mathbf{k}_0\mathbf{r}} + f(\theta,\varphi)\frac{e^{ik_0 r}}{r}\right] \tag{1}$$

where $f(\theta,\varphi)$ in first Born approximation is given by

$$f(\theta,\varphi) = -\frac{m_N}{2\pi\hbar^2}\int d^3r\, e^{i\mathbf{Q}\mathbf{r}} V(\mathbf{r}) \tag{2}$$

For low-energy and short-ranging (i.e. nuclear) interactions the potential $V(\mathbf{r})$ can well be approximated by the Fermi pseudo-potential [13]

$$V(\mathbf{r}) = \frac{2\pi\hbar^2}{m_N} b_j \delta^3(\mathbf{r}-\mathbf{r}_j) \tag{3}$$

thus that $f(\theta,\varphi)$ reduces to

$$f(\theta,\varphi) = -b_j \tag{4}$$

$b_j$ being the so-called atomic scattering length of atom $j$.

In this approximation, the differential scattering cross section per atom can be written as [14]

$$\frac{d\sigma}{d\Omega}(\mathbf{Q}) = \frac{1}{N}\left|f(\theta,\varphi)\right|^2 = \frac{1}{N}\left|\sum_{j=1}^{N} b_j \exp\left(\imath \mathbf{Q}\mathbf{r}_j\right)\right|^2 \tag{5}$$

where $N$ is the number of atoms exposed to the beam.

## *2.2 Magnetic scattering*

In the case of magnetic moments in the sample, the neutron undergoes a magnetic interaction in addition to the nuclear interaction. The corresponding interaction potential is given by [15]

$$V(\mathbf{r}) = -\boldsymbol{\mu}_N \cdot \mathbf{B}(\mathbf{r}) \quad \text{with} \quad \boldsymbol{\mu}_N = \gamma \frac{e\hbar}{2m_N}\boldsymbol{\sigma} \tag{6}$$

where $\boldsymbol{\mu}_N$ is the magnetic dipole moment of the neutron, $\boldsymbol{\sigma}$ the Pauli spin operator, $\gamma$ = -1.913 the gyromagnetic ratio and $\mathbf{B}(\mathbf{r})$ the magnetic field induced by an atom at the position of the neutron. The latter has two components, one induced by the magnetic dipole moment $\boldsymbol{\mu}_S$ of the electrons, denoted $\mathbf{B}_S(\mathbf{r})$, and one by their orbital moment $\boldsymbol{\mu}_L$, denoted $\mathbf{B}_L(\mathbf{r})$. The (weak) magnetic interaction $V(\mathbf{r}) = \boldsymbol{\mu}_N (\mathbf{B}_S(\mathbf{r}) + \mathbf{B}_L(\mathbf{r}))$ can as well be treated in first Born approximation, resulting in the magnetic scattering amplitude, in analogy to the nuclear scattering amplitude, given by the Fourier transform of the magnetic interaction potential

$$b_M = -\frac{m_N}{2\pi\hbar^2}\int d^3r\, e^{\imath \mathbf{Q}\mathbf{r}}\ \boldsymbol{\mu}_N \cdot \left(\mathbf{B}_S(\mathbf{r}) + \mathbf{B}_L(\mathbf{r})\right). \tag{7}$$

An additional static magnetic field $\mathbf{H}(\mathbf{r})$ at the point of local magnetization $\mathbf{M}(\mathbf{r})$ (originating from $\mathbf{B}_S(\mathbf{r}) + \mathbf{B}_L(\mathbf{r})$) induces a total local magnetic induction of

$$\mathbf{B}(\mathbf{r}) = \mu_0\left(\mathbf{H}(\mathbf{r}) + \mathbf{M}(\mathbf{r})\right) \tag{8}$$

and the Fourier transform of $\mathbf{B}(\mathbf{r})$ yields [cf. 16-18]

$$\mathbf{B}(\mathbf{Q}) = \mu_0 \frac{\mathbf{Q}\times\left[\mathbf{M}(\mathbf{Q})\times\mathbf{Q}\right]}{Q^2} = \mu_0 \mathbf{M}_\perp(\mathbf{Q}) = \mu_0 \mathbf{M}(\mathbf{Q})\sin\left(\angle(\mathbf{Q},\mathbf{M})\right) \tag{9}$$

where $\mathbf{M}(\mathbf{Q}) = \int d^3r \exp(i\mathbf{Q}\cdot\mathbf{r})\mathbf{M}(\mathbf{r})$, with $\mathbf{M}(\mathbf{r})$ given in units of Am.

$\mathbf{M}_\perp(\mathbf{Q}) = \mathbf{Q}\times\left[\mathbf{M}(\mathbf{Q})\times\mathbf{Q}\right]/Q^2 = \left|\mathbf{M}(\mathbf{Q})\right|\sin\left(\angle(\mathbf{Q},\mathbf{M})\right)$ is the magnetization component perpendicular to the scattering vector $\mathbf{Q}$. The magnetic scattering length then is [16]

$$b_M = \frac{\gamma e \mu_0}{2\pi\hbar}\boldsymbol{\sigma}\cdot\mathbf{M}_\perp(\mathbf{Q}) = D_M \mu_0 \boldsymbol{\sigma}\cdot\mathbf{M}_\perp(\mathbf{Q}). \tag{10}$$

For the differential scattering cross section one finally obtains

$$\frac{d\sigma_M}{d\Omega}(\mathbf{Q}) = \frac{D_M^2}{N}\left|\mu_0 \mathbf{M}_\perp(\mathbf{Q})\right|^2 \tag{11}$$

## 2.3 Polarized neutron scattering

In the presence of a preferred direction, for example induced by an external magnetic field, the magnetic scattering depends on the spin state $\boldsymbol{\sigma}$ of the neutrons. Let the z-axis be the preferred direction, and let (+) and (–) denote the neutron spin polarizations parallel and antiparallel to the z-axis, then the scattering is described by four scattering processes: two processes where the incident states (+) and (–) remain unchanged (++ and – –), the so-called 'non-spin-flip' processes, and two processes where the spin is flipped (+– and –+), the 'spin-flip' processes. Keeping in mind that the nuclear scattering does not flip the neutron spin, the four related scattering lengths are [19]

$$b_{\pm\pm} = b_N \mp D_M \mu_0 M_{\perp z} \tag{12a}$$

$$b_{\pm\mp} = -D_M \mu_0 \left(M_{\perp y} \pm i M_{\perp x}\right) \tag{12b}$$

It is evident that non-spin-flip scattering only contains magnetic contributions from effective magnetization components along the z-axis. If the scattering vector $\mathbf{Q}$ is parallel to the z-axis, $M_{\perp z}$ is zero. On the other hand, if spin-flip scattering is present, it is exclusively due to effective magnetic components deviating from the z-axis, the axis of magnetic polarization.

For an unpolarized neutron beam (which may be taken composed of 50% (+) and 50% (–) polarization) the square of the modulus of the scattering length is

$$\left|b\right|^2 = \frac{1}{2}\left(b_{++}^2 + b_{--}^2 + \left|b_{+-}\right|^2 + \left|b_{-+}\right|^2\right) = b_N^2 + D_M^2\left|\mu_0 \mathbf{M}_\perp\right|^2 \tag{13}$$

The differential cross section of the unpolarized neutron beam can therefore be described by the sum of the nuclear and the magnetic cross section, without any cross terms.

## 2.4 Small angle neutron scattering

### 2.4.1 Scattering by individual magnetic particles

Small angle scattering does not resolve individual atoms, but structures of sizes in the nanometer range. Therefore the discrete atomic scattering lengths $b_j$ can be replaced by a scattering length density $\rho(\mathbf{r})$ of the sample. The differential scattering cross-section (c.f. Eq. (5)) is than given by the Fourier transform of $\rho(\mathbf{r})$:

$$\frac{d\sigma}{d\Omega}(\mathbf{Q}) = \frac{1}{V}\left|\int_V d^3r\,\rho(\mathbf{r})e^{i\mathbf{Q}\cdot\mathbf{r}}\right|^2 \tag{14}$$

with $V$ being the sample volume. Assuming that this volume contains $N$ particles embedded in a surrounding matrix of constant scattering cross section $\rho_{\text{matrix}}$ , we define the scattering length distribution inside each particle by $\rho_{P,j}(\mathbf{r})=\Delta\eta_j(\mathbf{r})+\rho_{\text{matrix}}$ . Than, with $\mathbf{R}_j$ being the vector pointing to the centre of the particle $j$, the related scattering cross section can be written as

$$\frac{d\sigma}{d\Omega}(\mathbf{Q}) = \frac{1}{V}\left|\sum_{j=1}^{N} F_j(\mathbf{Q})\,e^{i\mathbf{Q}\mathbf{R}_j}\right|^2 \quad \text{with} \quad F_j(\mathbf{Q}) = \int_{V_j(\mathbf{R}_j)} d^3r\,\Delta\eta_j(\mathbf{r})\; e^{i\mathbf{Q}(\mathbf{r}-\mathbf{R}_j)} \tag{15}$$

For particles of constant scattering length density, the scattering amplitude for nuclear scattering can be expressed as

$$F_N(\mathbf{Q}) = \Delta b_N V_P\, f(\mathbf{Q}). \tag{16}$$

where the constant $\Delta\eta_j$ was replaced by $\Delta b_N$ , the contrast for nuclear scattering between the particles and the surrounding matrix. $V_P$ is the particle volume. $f(\mathbf{Q})$ denotes the so-called particle formfactor and can be calculated analytically for many simple particle shapes, as tabulated in [20]. For spherical particles of radius $R$, it is the well-known expression, dating back to Lord Rayleigh [21]

$$f(QR) = 3\frac{\sin(QR) - QR\cos(QR)}{(QR)^3}. \tag{17}$$

We now assume the same particles being of homogenous magnetisation $\mathbf{M}_P$, embedded in a homogenously magnetized surrounding $\mathbf{M}_M$. The magnetic scattering of these particles then depends on the magnetic contrast vector $\Delta\mathbf{M}= \mathbf{M}_P-\mathbf{M}_M$ relative to the scattering vector $\mathbf{Q}$:

$$\mathbf{M}_\perp = \frac{\mathbf{Q}\times(\Delta\mathbf{M}\times\mathbf{Q})}{Q^2} \tag{18}$$

To calculate the magnetic scattering amplitude one has to consider the spin state before and after the scattering process according to Eqs. (12a,b)

$$F_{\pm\pm}(\mathbf{Q}) = \Delta b_{\pm\pm} V_P\, f(\mathbf{Q}), \qquad F_{\pm\mp}(\mathbf{Q}) = \Delta b_{\pm\mp} V_P\, f(\mathbf{Q}) \tag{19}$$

### *2.4.2 Scattering by groups of particles*

The scattering from an accumulation of many particles is obtained by summing up the scattering amplitudes of all particles weighted by a phase shift at each particle position. The general expression for the scattering cross section then is given by

$$\frac{d\sigma_j}{d\Omega}(Q) = \left\langle F_j^2(Q)\right\rangle + \left\langle F_j(Q)\right\rangle^2 (S(Q)-1) \tag{20}$$

(*j* standing for $\pm\pm, \pm\mp$, or N and M in the case of unpolarized neutrons, respectively). The right-hand-side of Eq. (20) consist of two terms: The first one depends only on the particle structure and corresponds to the independent scattering of *N* particles, while the second one considers their spatial distribution and reflects the interparticle interference described by $S(\mathbf{Q})$. The $\langle\ \rangle$ indicates an average over all possible configurations and sizes of the particles.

As postulated by Eq. (13), in the case of an unpolarized incident neutron beam the scattering of both contributions, nuclear and magnetic, is linearly superposed

$$\frac{d\sigma_{unp}}{d\Omega}(\mathbf{Q}) = \frac{d\sigma_N}{d\Omega}(\mathbf{Q}) + \frac{d\sigma_M}{d\Omega}(\mathbf{Q}) \tag{21}$$

In both contributions two averages are involved: the average of the squared scattering function and the square of the average scattering function. For monodisperse, radially symmetric particles, for nuclear scattering the averages $\left\langle F_N^2(Q)\right\rangle \equiv \left\langle F_N(Q)\right\rangle^2$ are identical, so that

$$\frac{d\sigma_N}{d\Omega}(Q) = F_N^2(Q)S(Q) \tag{22}$$

To evaluate the averages for the magnetic scattering cross-section we have to consider the angular orientations of $\Delta\mathbf{M}$, parameterized by the angular alignment probability $p(\varphi_M, \Theta_M)$ of $\Delta\mathbf{M}$. Following up Eq. (11), the averages over all $p(\varphi_M, \Theta_M)$ are than given by the general expressions

$$\left\langle F_M^2(Q)\right\rangle = V_P^2 f^2(Q,R)\int p(\varphi_M,\Theta_M)[D_M\mu_0\mathbf{M}_\perp(\mathbf{Q})]^2 d\varphi_M d\Theta_M \tag{23a}$$

$$\left\langle F_M(Q)\right\rangle^2 = \left[\int p(\varphi_M,\Theta_M)V_P f(Q,R)D_M\mu_0\mathbf{M}_\perp(\mathbf{Q})d\varphi_M d\Theta_M\right]^2 \tag{23b}$$

For two extremes, i.e. a demagnetised sample ($\Delta\mathbf{M}$ at random orientation) and a sample in magnetic saturation ($\Delta\mathbf{M}$ all parallel), the averages can readily be performed:

In the case of random orientation of $\Delta\mathbf{M}$ the square of the average formfactor $\left\langle F_M(\mathbf{Q})\right\rangle^2$ is zero and

$$\frac{d\sigma_M}{d\Omega}(\mathbf{Q}) = \left\langle F_M^2(\mathbf{Q})\right\rangle = \frac{2}{3}(D_M\mu_0\Delta M)^2 V_P^2 f^2(\mathbf{Q}) \tag{24}$$

which is independent of interparticle interference effects.

In the case of magnetic saturation, the averages $\left\langle F_M^2(\mathbf{Q})\right\rangle \equiv \left\langle F_M(\mathbf{Q})\right\rangle^2$ are identical, as for nuclear scattering, and we obtain

$$\frac{d\sigma_M}{d\Omega}(\mathbf{Q}) = (D_M \mu_0 \Delta M)^2 V_P^2 f^2(\mathbf{Q}) \sin^2(\Psi) \tag{25}$$

where $\Psi = \angle(\mathbf{Q}, \Delta\mathbf{M})$, the angle between the direction of the magnetic contrast $\Delta\mathbf{M}$, and the scattering vector ***Q***, in practice the azimuthal angle on the two-dimensional SANS detector.

Averaging with regard to the azimuthal angle results in

$$\frac{d\sigma_M}{d\Omega}(\mathbf{Q}) = \frac{1}{2}(D_M \mu_0 \Delta M)^2 V_P^2 f^2(\mathbf{Q}) \tag{26}$$

which differs from Eq (24) only by the prefactor 1/2 instead of 2/3.

If the particles are not monodisperse in size, and/or not equal in shape, each size/shape class has to be considered individually. When interparticle interference can be neglected, the scattering contributions of the different classes are incoherently superposed. In the particular case of a finite size distribution of equally shaped particles, neglecting interparticle interference, the scattering cross section can be calculated as the integral over all individual contributions from the size interval between *R* and *R* + *dR*. For the nuclear scattering, this results in

$$\frac{d\sigma_N}{d\Omega}(\mathbf{Q}) = \Delta b_N^2 \int_R f^2(\mathbf{Q}) V_P^2(R) N(R) dR \tag{27}$$

with $N(R)\, V_P(R)\, dR$ being the incremental volume fraction with $V_P(R)$, the particle volume in the related size interval.

For the magnetic scattering of particles of finite size distribution and in magnetic saturation, the scattering cross section is given in analogy to Eq. (27) by

$$\frac{d\sigma_M}{d\Omega}(\mathbf{Q}) = (D_M \mu_0 \Delta M)^2 \sin^2\Psi \int_R f^2(\mathbf{Q}) V_P^2(R) N(R) dR \tag{28}$$

# 3. Experiment description

The aim of this experiment is to measure the nuclear and magnetic scattering of a ferromagnetic structure. The scattering will be measured at different magnetic fields, zero field, intermediate field and saturating field. If available also polarised neutrons will be used. The magnetic field will be always perpendicular to the incoming neutron beam direction.

## 3.1 Samples

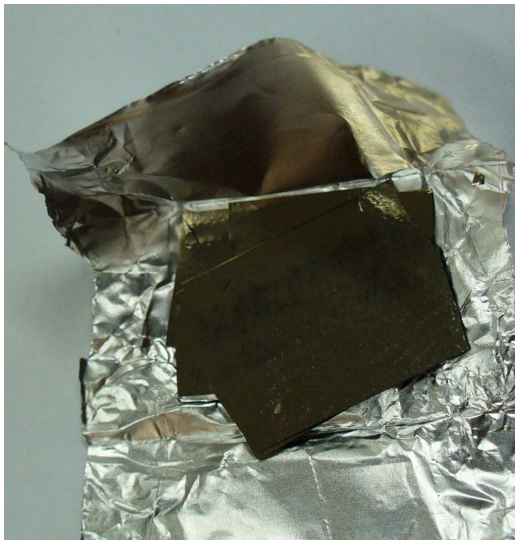

softmagnetic nanocrystalline metallic ribbons: $Fe_{73.5}Si_{15.5}B_7Nb_3Cu_1$

superparamagnetic Co precipitates in a Cu matrix

Two different alloy will be measured in this practical. A very soft magnetic nanocrystalline alloy and Co precipitates in a Cu matrix showing superparamagnetic behaviour.

### 3.1.1 Finemet – FeSiBNbCu

Nanocrystalline materials of the FeSiBNbCu system are well known for their soft magnetic properties, i.e. high permeability, low coercivity and low magnetostriction. They are prepared from the melt spun amorphous alloy by thermal treatment: Annealing at 823 K for 1.5h produces nano-sized α-Fe(Si) crystallites of about 5 nm in radius embedded in an amorphous matrix. The excellent soft magnetic properties of these materials have attracted much attention for structural and magnetic studies. It is known that the combined addition of copper and niobium to the amorphous Fe-Si-B alloy is crucial for the formation of the nanostructured morphology: Whereas the addition of Cu enhances the nucleation of α-Fe(Si) grains, the slow-diffusing Nb hinders a rapid growth.

### *3.1.2 Solid superparamagnetic CuCo system*

CuCo alloys containing 0.8 at.% Co decompose by annealing and build precipitates of fcc-Co α-phase. The specimen was prepared by levitation melting in an induction furnace. A chemical analysis confirmed the nominal composition within ± 0.02 at.%. The ingots were cold-rolled to foils of 1 mm thickness and cut into squares of 10x10 $mm^2$. The foil was than solution treated at 1223 K for 3 h under argon atmosphere, followed by a rapid quench into water at room temperature. Afterwards the quenched sample was annealed at 793 K for 40 minutes in a three-zone furnace under argon atmosphere. The system CuCo is known to form spherical precipitates of Co-rich α phase containing about 90 at.% Co, dispersed in a matrix of almost pure Cu. In this system small ferromagnetic Co precipitates are formed in a non-magnetic Cu matrix during aging showing superparamagnetic properties. The size and volume fraction can be controlled by the initial composition and the annealing procedure. For the chosen system of Cu 0.8at.%Co and an annealing at 793K for 40 min we find precipitates around 5nm radius with a narrow size distribution.

## *3.2 Experimental Setup*

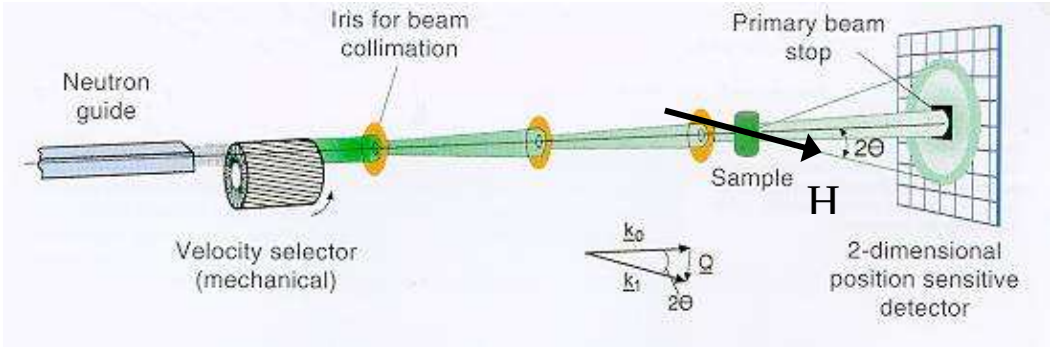


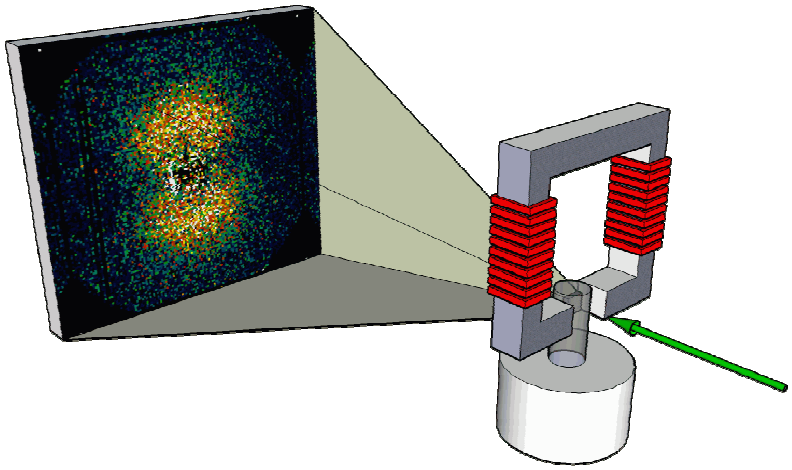

An electromagnet is used to apply a horizontal magnetic field perpendicular to the incoming neutron beam. For the measurements a neutron wavelength between 0.6 and 1.2 nm should be used. SANS data will be taken at different detector distances and collimation lengths ranging from 2m to 18m. For each setting a reference measurement with an empty sample holder has to be taken. Furthermore for the 6 and 2 m detector distances water has to be measured for absolute calibration and detector efficiency correction. The transmission of the samples will be measured at 18 m detector distance. The data correction can be done either with the software package "Grasp" from the ILL or the "BerSANS" program from the HZ Berlin.

## *3.3 Tasks*

1. The electromagnet is not calibrated. Before the experiment you have to measure a hysteresis curve to know the magnetic field as a function of the current.
2. Make an experimental plan, i.e. decide which wavelength and detector and collimation settings you want to use.
3. Decide at which magnetic fields you like to do experiments.
4. Perform short test measurements to see how long you have to measure at each setting.
5. Try to write a batch file for automatic data acquisition, if possible.
6. Carry out the full 2-dimensional data correction.
7. Separate the nuclear from the magnetic scattering if possible.
8. Depending whether a spin flipper is available or not also spin dependent scattering pattern will be taken.
9. Try to find a model for describing the scattering pattern.
10. Cross check for the Co precipitates if the intensities for nuclear and magnetic scattering are consistent with the nuclear scattering contrast and bulk magnetization of Co.

## *3.4 Recommended readings*

A very good summary about small angle scattering are given in

- Structure Analysis by Small-Angle X-Ray and Neutron Scattering, L.A. Feigin and D.I Svergun, Plenum Press 1987
- Neutrons, X-rays and Light: Scattering Methods Applied to Soft Condensed Matter, edited by P. Lindner and Th. Zemb, North Holland, 2002

A good summary about magnetic small angle neutron scattering can be found in

- A. Wiedenmann, Magnetic and crystalline nanostructures in ferrofluids as probed by small angle neutron scattering, Ed. S. Odenbach, Ferrofluids, published in the Springer Serie: Lecture Notes in Physics
- A. Wiedenmann, Small Angle Neutron Scattering Investigations of Magnetic Nanostructures, Chapter 10, Ed. Tapan Chatterji, Neutron Scattering from Magnetic Materials, Elsevier 2006

# *4. References*


[1] V. F. Sears, Neutron News **3** (1992) 26, L. Koester, H. Rauch, M. Herkens, K. Schröder, Report of the Research Centre Jülich (FZJ), Germany, ISSN 0366-0885, IAEA-Contract 2517/RB (1981), G.E.Bacon, 'Neutron Diffraction', Clarendon Press, Oxford (1975)

[2] CRC Handbook of Chemistry and Physics, ed. R. C. Weast, CRC Press, Florida, E-107

[3] C.G. Shull and M.K. Wilkinson, Phys. Rev. **97** (1955) 304

[4] K. Ibel, J. Appl. Cryst. **9** (1976) 296

[5] H. R. Child, S. Spooner, J. Appl. Cryst. **13** (1980) 259

[6] J. Kohlbrecher and W. Wagner, J. Appl. Cryst **33** (2000) 804

[7] T. Keller, T. Krist, A. Danzig, U. Keiderling, F. Mezei, A. Wiedenmann, Nuclear Instruments and Methods in Physics Research A 451 (2000) 474-479

[8] J. Zhao, W. Meerwinck, T. Niinikoski, A. Rijllart, M. Schmitt, R. Willumeit and H. Stuhrmann, Nuclear Instruments and Methods in Physics Research A 356 (1995) 133-137

[9] H. Glättli, M. Eisenkrämer, M. Pinot and C. Fermon, Physica B 213&214 (1995) 887-888

[10] P. Thiyagarajan, J. E. Epperson, R. K. Crawford, J. M. Carpenter, T. E. Klippert and D. G. Wozniak, J. Appl. Cryst. **30** (1997) 280

[11] O. Hittmair, "Lehrbuch der Quantentheorie", Karl Thiemig publishing (1972)

[12] J. Byrne, Neutrons, Institute of Physics Publishing, Bristol (1994), Chap. 2

[13] E. Fermi, Ric. Sci **7** (1936) 13

[14] G. Kostorz and S.W. Lovesey, in Treatise on Materials Science and Technology (Vol. **15**: Neutron Scattering), edited by G. Kostorz, Academic Press, New York, 1979, 22

[15] J. Rossat-Mignot, Neutron Scattering, Vol **23**, Part C (1997) Academic Press

[16] G.L. Squires, Cambridge University Press (1978)

[17] I.I. Gurevich and L.V. Tarasov, North Holland Publishing Company, Amsterdam (1968)

[18] W. Schmatz, in Treatise on Materials Science and Technology (Vol. 2), edited by H. Herman Academic Press, New York (1973), 128

[19] R.M. Moon, T. Riste, W.C. Koehler, Phys. Rev. **181** (1969) 920

[20] J.S. Pedersen, Advances in Colloid and Interface Science **70** (1997) 171

[21] O. M. Lord Rayleigh, Proc. R. Soc. London, A **84** (1911) 25